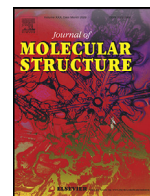




ELSEVIER

Contents lists available at ScienceDirect

Journal of Molecular Structure

journal homepage: www.elsevier.com/locate/molstr

The quest for a better understanding of ethanol coordination to magnesium and zinc porphyrin: A combined experimental and theoretical study

Bishnu Prasad Borah, Smita Majumder, Karishma Devi Borah, Jagannath Bhuyan*

Department of Chemistry, North Eastern Regional Institute of Science and Technology (NERIST), Nirjuli, Arunachal Pradesh, 791109, India

ARTICLE INFO

Article history:

Received 14 September 2020

Revised 22 October 2020

Accepted 11 November 2020

Available online xxx

Keywords:

Porphyrin

magnesium

density functional theory

Hirshfeld surface analysis

crystal structure

ABSTRACT

An ethanol coordinated magnesium porphyrin [Mg(TDMPP)(C₂H₅OH)], (TDMPP = 5,10,15,20-tetrakis(3,5-dimethoxyphenyl)porphyrin), **1** was synthesized and characterized by single crystal X-ray diffraction method along with other standard spectroscopic techniques. This is the first known crystal structure of an alcohol bound magnesium porphyrin of tetraphenylporphyrin derivatives. Crystal structure of the compound shows a weak hydrogen bonding interaction (2.730(4) Å) between OH group of axial ethanol molecule and a peripheral methoxy group of an adjacent porphyrin molecule. This hydrogen bonding results the formation of a weak one-dimensional supramolecular structure. The fluorescence and electrochemical studies have also been performed. To explore the disadvantages of using zinc porphyrins to study chlorophyll type magnesium porphyrins, a comparison of theoretical study using DFT level was performed between compound [Mg(TDMPP)(C₂H₅OH)], **1** and its zinc counterpart [Zn(TDMPP)(C₂H₅OH)], **2**. Theoretical calculations include optimization of geometry, energy of frontier molecular orbitals (FMOs), electronic transitions and global chemical indices. The global reactivity indices like η , μ and ω derived from theoretical calculations for zinc and magnesium porphyrin supports that magnesium porphyrin is more reactive than the zinc analogue. Furthermore, the Hirshfeld surface analysis was used to quantify the weak intermolecular interactions present in the crystal lattice of compound **1**.

© 2020 Elsevier B.V. All rights reserved.

Introduction

The synthetic magnesium porphyrins have attracted significant interest recently due to their application in different fields such as sensors [1], catalyst [2,3], antibacterial properties [4], determination of absolute configuration of monoalcohols [5] etc., besides the relevance with chlorophyll molecules in photosynthesis [6–10]. In spite of so many importance magnesium porphyrins known in the literature is very less compared to other similar porphyrins like zinc because in the early time of porphyrin research (owing to the synthetic difficulties of magnesium porphyrins) zinc porphyrins were used to model chlorophyll type molecules. The study of axial coordination of small molecules or anions to magnesium porphyrins is an exciting topic as a water molecule is usually present in the chlorophyll molecules in the green leaves. The axial coordination of small molecules, anions, and coordination from the peripheral groups of same or different compounds are thoroughly studied for zinc porphyrins [11–13]. Similar studies are also very

limited with magnesium porphyrins and the study of zinc porphyrin was considered as model for chlorophyll type molecules. A penta-coordinated magnesium porphyrin is known which shows enhanced fluorescence intensity in the presence of cholesterol [14]. Fiedor and coworker carried out theoretical calculation at the DFT level to understand water coordination in magnesium tetrapyrroles and other chelates and found that the binding between Mg²⁺ and water is primarily electrostatic in nature and coordination number is reduced from six to five as the binding of water in the sixth site does not result any energy gain [15]. The one dimensional coordination polymer of magnesium 3,4,5-trimethoxyphenylporphyrin (due to metal-oxygen linking between *meta*-methoxy group of two adjacent porphyrins) [16], [Mg^{II}(TPBP)(4,4'-bpy)₂] (TPBP = (5,10,15,20-tetrakis[4-(benzoyloxy)phenyl]porphyrin), (4,4'-bpy = 4,4'-bipyridine) [17], supramolecular chain network of diaqua(5,10,15,20-tetraphenylporphyrinato-k⁴N)magnesium-18-crown-6, [MgTPP(H₂O)₂](18-C-6) [18], and [MgT(*p*-OME)PP(H₂O)] [19] are known. Magnesium tetranitrooctaethylporphyrin is found to form similar type of one-dimensional polymeric chains with different bidentate axial ligands like pyrazine or cyanopyridine [20]. Using non-covalent interactions Coutsolelos and coworkers

* Corresponding author.

E-mail address: jnb@nerist.ac.in (J. Bhuyan).

designed a supramolecular donor–acceptor conjugates to model of photosynthetic systems [21]. We and others have studied the ethanol coordination to zinc porphyrins [22–24]. Though it is known that alcohols can bind to magnesium porphyrins very easily, to the best of our knowledge crystal structure of magnesium porphyrin with a bound alcohol type molecule is not known in the literature. Therefore, here we have reported the synthesis, structural characterization of an axially ethanol coordinated magnesium porphyrin, [Mg(TDMPP)(C₂H₅OH)] and to understand profoundly the difference between magnesium and zinc porphyrins, a theoretical study of magnesium porphyrin [Mg(TDMPP)(C₂H₅OH)], **1** and its zinc analogue, [Zn(TDMPP)(C₂H₅OH)], **2** have been undertaken. The Hirshfeld surface analysis [25] and 2D fingerprint plots have been studied to understand the different types of interactions present in the crystal lattice.

Experimental

General considerations

All the reagents used in the experiments were of analytical grade and used without any further purification. Dichloromethane, hexane, chloroform, magnesium acetate and N,N dimethylformamide were obtained from Merck Life Science Private Limited. 3,5-Dimethoxybenzaldehyde and pyrrole were purchased from Spectrochem Private Limited. Ethanol and propionic acid were purchased from SRL.

Physical Measurements

UV-Visible spectra were recorded in a Perkin-Elmer (Lambda 35) spectrophotometer. A Shimadzu FT-IR spectrophotometer (IR affinity) was used for acquiring Infra-Red spectra at 400–4000 cm⁻¹ range using pressed KBr disks. Luminescence spectral measurements were acquired using an Agilent Cary Eclipse Fluorescence Spectrophotometer. Elemental analysis for carbon, hydrogen and nitrogen were analyzed with Leco CHNOS 948 carbon hydrogen nitrogen oxygen determination. An electrochemical workstation CH instrument CHI600E was used for cyclic voltammetry (CV) experiments. Three electrode systems consist of glassy carbon electrode as working electrode, Pt electrode as auxiliary electrode and Ag/AgCl electrode as reference electrode were used in dichloromethane medium in nitrogen atmosphere for electrochemical measurements.

X-ray structural analysis

A suitable crystal of the magnesium porphyrin was used for data collection in a Bruker APEX-II CCD diffractometer. The instrument was equipped with CCD area detector and data were collected using graphite-monochromated Mo K α radiation ($\lambda = 0.71073$ Å) at room temperature (293K). All empirical absorption correction was applied using the SADABS program. All data were acquired with Bruker APEX2 and were integrated with the BRUKER SAINT program. SIR97 was used for solving and SHELXS-97 (Sheldrick 2008) for refining the structure. The space group of the compound was determined based on the lack of systematic absence and intensity statistics. Full matrix least squares/difference Fourier cycles have been performed which located the non-hydrogen atoms. All non-hydrogen atoms were refined with anisotropic displacement parameters. Hydrogen atom attached to oxygen of ethanol molecule was located from difference Fourier map and refined isotropically. The structural figures were drawn with the Olex2 [26].

Theoretical studies

The theoretical calculations like optimization of structures, Frontier Molecular Orbitals (FMO) energy calculation, simulation of UV-VIS spectrum of compound were performed at DFT level using Gaussian16 [27] software using the basis set LANL2DZ [28] along with functional B3LYP [29,30]. The UV-VIS spectrum of compound was simulated using TD-DFT method and compared with the experimental result. The initial geometries were taken from crystal structure of compounds. For compound **2**, the initial geometry was taken from the crystal structure reported by Bhyappa and coworkers [31]. Hirshfeld surface analysis and fingerprint plots were performed using crystal explorer software [32].

Synthesis of ligand 5,10,15,20-tetrakis(3,5-dimethoxyphenyl)porphyrin (H₂TDMPP)

The ligand 5,10,15,20-tetrakis(3,5-dimethoxyphenyl)porphyrin (H₂TDMPP) was synthesized according to the method of Adler and Longo [33]. A sample of 8.75 mL (0.144 mmol) of 3,5 dimethoxybenzaldehyde was refluxed for one hour with 5 mL (0.144 mmol) pyrrole in 250 mL propionic acid. The solution was then allowed to cool and kept for further 24 hours. Then the dark solid residue was collected by filtration and was washed with water and ethanol and allowed for air dry. The yield of the compound was 1.68 g (20%). Molecular formula of the ligand is C₅₂H₄₆N₄O₈; Molecular weight 854; UV/Vis (CHCl₃, 10⁻⁵M) λ_{\max} , nm (ϵ , mol⁻¹dm³cm⁻¹): 420 (348000), 516(22000), 547(8000), 590 (7200), 646 (5600).

Synthesis of compound [Mg(TDMPP)(C₂H₅OH)], **1**

A sample of 1g (1.02 mmol) of H₂TDMPP and 2 g (4.07 mmol) of magnesium-acetate, Mg(CH₃COO)₂ was warmed in 120 mL DMF for one hour then a small amount of (0.2g) sodium acetate was added. The final solution was refluxed for 7 hrs. The solvent was removed by slow evaporation by keeping the solution mixture on water bath. The crude product was dissolved in dichloromethane, filtered and evaporated using rotary evaporator. Finally, column chromatography (neutral alumina) using solvent mixture of dichloromethane and hexane was used for isolation and purification of the product. The compound was re-crystallized using a chloroform-hexane mixture with trace amount of ethanol. The yield of compound [Mg(TDMPP)(C₂H₅OH)] was 80%. Molecular Formula: C₅₄H₅₀MgN₄O₉; Molecular Weight 923.29; Elemental analysis (%) calcd. for C₅₄H₅₀MgN₄O₉: C 70.25, H 5.46, N 6.07; found C 70.50, H 6.28, N 6.21. UV/Vis (CHCl₃) λ_{\max} , nm(ϵ , mol⁻¹dm³cm⁻¹): 424 (600000), 553 (28000), 603 (8000). IR analysis give important peaks at 3410($\nu_{\text{O-H}}$), 2923($\nu_{\text{aromatic C-H}}$), 1736($\nu_{\text{C=N}}$), 1597($\nu_{\text{C=C}}$), 1463($\nu_{\text{C=C, pyrrole}}$), 1353($\nu_{\text{C-N}}$), 1161($\nu_{\text{C-H, pyrrole}}$), 1072($\nu_{\text{C-O-C}}$), 844($\nu_{\text{methane C-H}}$) and 755($\nu_{\text{N-H out-of-plane deformation}}$) cm⁻¹ respectively. The IR spectrum of the compound **1** is shown in supplementary information as Fig S1

Result and discussion

Crystal structure

A simple and effective magnesium metalation to porphyrin type molecules was developed by Lindsey and co-workers [34]. An axially coordinated water molecules is usually seen in the crystal structure of chlorophyll type molecules [35,36] which results a hydrogen bonding interaction between axial water molecule and peripheral methyl ester carbonyl oxygen atom in chlorophyll molecules [37,38]. The hydrogen bonding may have some role in

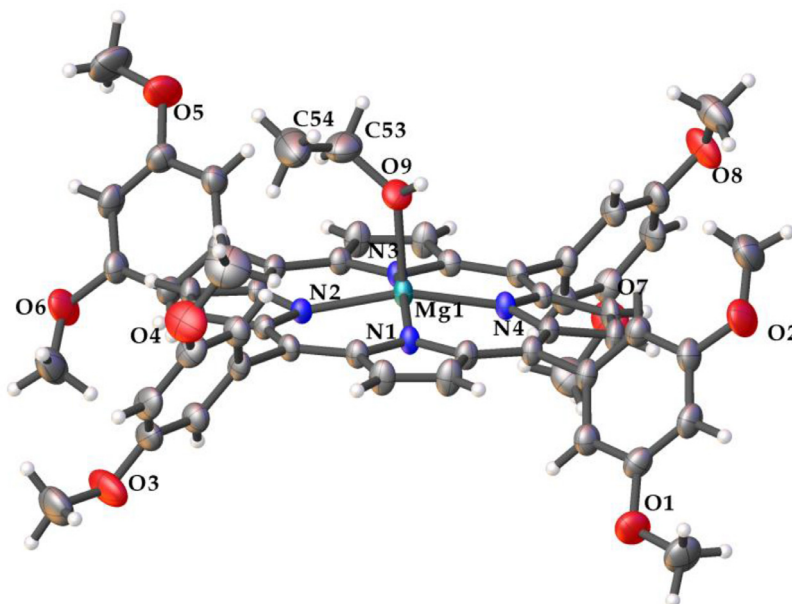


Fig. 1. Perspective view of compound [Mg(TDMPP)(C₂H₅OH)].

the energy dissipation process of photosynthesis. The suitable crystal for single crystal X-ray diffraction studies of compound **1** was obtained from DCM-ethanol-hexane mixture. The compound crystallized in a monoclinic crystal system with $P2_1/C$ space group and the perspective view of the compound is given in the Fig. 1. In the complex **1**, the metal magnesium is positioned at a distance of 0.322 Å above the porphyrin plane with Mg-N(py) bond length are between 2.075 to 2.080 Å [Mg1-N1=2.080(2), Mg1-N2=2.075(2), Mg1-N3=2.076(2), Mg1-N4=2.079(2)], which agrees well with known Mg-N(py) bond length of magnesium porphyrins [16,39]. The axial Mg-O (ethanol) bond distance is found as 2.079(2) Å which is in the range of all Mg-O bond distance of reported magnesium porphyrins [15,40]. A hydrogen bonding interaction between OH group of the axial ethanol molecule and a peripheral methoxy groups of a neighbouring porphyrin molecule, and another similar hydrogen bonding interaction between a peripheral methoxy groups and axial ethanol molecule of another neighbouring porphyrin makes the compound **1** as a weak one-dimensional hydrogen bonded supramolecular structure (Fig. 2). The hydrogen bonding distance between the methoxy oxygen atom and axially linked ethanol molecule is 2.730(4) Å. Although, it is very much challenging to locate hydrogen atoms (as only one electron is present) using X-ray diffraction [41–42] we could locate the hydrogen atom attached to oxygen of ethanol molecule from difference Fourier map and refined isotropically. All the bond lengths and bond angles of bound ethanol are within the normal ranges [43]. Moreover, the position and bond length of H attached to oxygen (ethanol) of the geometry optimized structure O-H (0.977 Å) corroborates the position of H of the single crystal data [O-H (0.92(5) Å].

The packing diagram of the compound **1** is given in the supplementary information Figure S2. The crystallographic data for the complex [Mg(TDMPP)(C₂H₅OH)] is given in Table 1.

UV-visible and Luminescence studies

The UV-visible spectrum of the compound [Mg(TDMPP)(C₂H₅OH)] shows a typical Soret band (at 425 nm) and two Q bands (in the range 550–600 nm), arises due to porphyrin $\pi-\pi^*$ electronic transition [44]. The electronic spectra of free base porphyrin H₂TDMPP and magnesium porphyrin

Table 1

Crystallographic data^a for complex [Mg(TDMPP)(C₂H₅OH)].

Complex	[Mg(TDMPP)(C ₂ H ₅ OH)]
Chemical Formula	C ₅₄ H ₅₀ MgN ₄ O ₉
Formula weight	923.29
Crystal system	Monoclinic
Space group	$P2_1/C$
Temperature (K)	293
<i>a</i> , <i>b</i> , <i>c</i> (Å)	24.437(5), 8.792(5), 22.912(5)
α , β , γ	90.000(5) [°] , 109.384(5) [°] , 90.000(5) [°]
<i>h</i> , <i>k</i> , <i>l</i> _{max}	33, 12, 31
<i>V</i>	4644(3) Å ³
<i>Z</i>	4
Radiation Type	Mo $K\alpha$
Wavelength (Å)	0.71069
Completeness	0.997
Absorption coefficient	0.102 mm ⁻¹
<i>d</i> _{calcd}	1.321 gcm ⁻³
Data collection diffractometer	Bruker APEX-II CCD diffractometer
Absorption correction	SADABS (Bruker, 2002)
No. of reflections collected/ unique	90289/12369
<i>R</i> _{int}	7.12%
<i>R</i> indices	^b <i>R</i> ₁ = 9.15 %, ^c <i>wR</i> ₂ = 22.25 %
<i>S</i> (Goodness of fit)	1.16
Deposition number	CCDC 1984143

^aMo $K\alpha$ radiation.

^b $R_1 = \frac{\sum ||F_o| - |F_c||}{\sum |F_o|}$.

^c $wR_2 = \left\{ \frac{\sum [w(F_o^2 - F_c^2)^2]}{\sum [w(F_o^2)^2]} \right\}^{1/2}$.

[*Z*- no. of formulae units per unit cell; *a*, *b*, *c*- length of the cell edges; *V*- volume of the unit cell; *d*_{calcd}- density of unit cell calculated].

[Mg(TDMPP)(C₂H₅OH)] is presented in supporting information Figure S3. The ethanol bound zinc porphyrin showed a red shift of Soret and Q bands from ethanol free parent porphyrin due to the axial ligation of the ethanol molecule which brings the metal out of the porphyrin plane and alters the symmetry and energetic distribution of frontier molecular orbitals [22,34]. The UV-visible spectroscopic data of some of known similar compounds are given in Table 2.

There are reports of formation of isoporphyrins from zinc porphyrin upon addition of oxidizing agents such as ceric ammonium nitrate in nucleophilic solvents [22,45–48]. To understand the generation of similar type of compounds from magnesium porphyrin

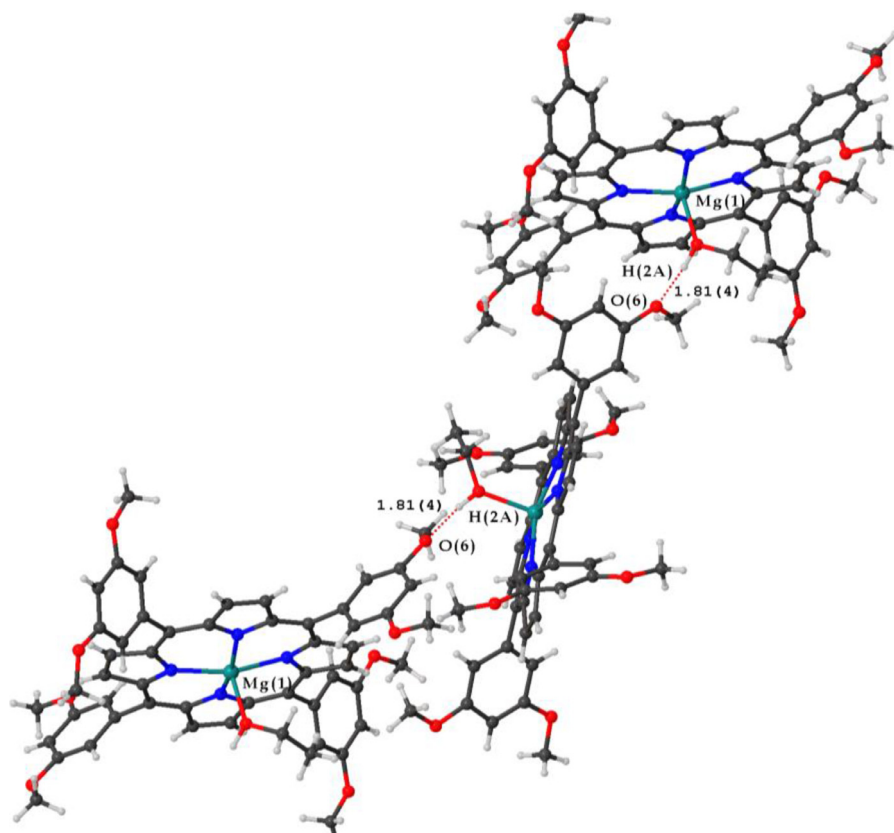


Fig. 2. Intermolecular H-bonding interaction present in compound $[\text{Mg}(\text{TDMPP})(\text{C}_2\text{H}_5\text{OH})]$.

Table 2
UV/Vis data of some Mg porphyrins.

Compound	Solvent	Soret band λ [nm]	Q bands λ [nm]	Reference
$[\text{Mg}(\text{TDMPP})(\text{C}_2\text{H}_5\text{OH})]$	Chloroform	424	553,603	This paper
$[\text{Mg}(\text{TPP})(\text{THF})_2]$	Toluene	426	524,564, 604	40
$[\text{Mg}(\text{TPP})(\text{H}_2\text{O})]$	Chloroform	423	563,602	35
$[\text{MgTPP}(\text{C}_{60}\text{Im})]$	Benzene	405	568, 608	9
$[\text{Mg}(\text{TMPP})(\text{H}_2\text{O})]$	Dichloromethane	428	563,603	14

we have added ceric ammonium nitrate to a solution of the magnesium porphyrin **1**. Upon addition of ceric ammonium nitrate and other oxidizing agents, the electronic spectrum changes immediately with the appearance of two peaks in the lower energy region of electronic spectrum (700–900 nm) and simultaneous decrease of the intensity of Soret band. But, the electronic spectrum within a couple of minutes changes to spectrum of porphyrin acid dication (Supporting Information Figure S4) may be due to demetallation. The isolation and full characterization of the intermediate isoporphyrin type species was not successful even when used in a basic solution to stop the demetallation. It is known that magnesium porphyrin undergoes demetallation even in the trace amount of acidic water [34]. The electronic spectra of magnesium porphyrin and the intermediate with strong absorbance similar to isoporphyrin type species is shown in Fig. 3. It displayed the Soret peak at 430 nm whereas the two Q bands appeared at 765 and 858 nm.

The luminescence properties were studied in dichloromethane solution at two different concentrations. The compound was found to show two well-defined emission peaks at 608 and 661 nm (Fig. 4) when excited at Soret band for (Q(0,0)) and (Q(0,1)) respectively which is good agreement with emission peaks of other Mg-porphyrins found in the literature [15,49]. The intensity of luminescence spectrum at higher concentration (10^{-4} M) was found

very less (Fig. 4) compared to dilute solution (10^{-6} M). This lower intensity at higher concentration may be due to the effect of concentration quenching observed for zinc porphyrins [46,50]. Mg-porphyrins show higher quantum yield than corresponding Zn-porphyrins and free base porphyrins due to its longer excited state lifetime [51–53]. Recently, we have determined the quantum yield of a zinc isoporphyrin and found that isoporphyrin have lower value of quantum yield than parent zinc porphyrin due to the loss of macrocyclic aromaticity [22].

Electrochemistry

Electrochemical measurements were carried out using cyclic voltammetry three electrode system to measure the redox potential of compound $[\text{Mg}(\text{TDMPP})(\text{C}_2\text{H}_5\text{OH})]$ in dichloromethane medium. Similar to zinc porphyrins, magnesium porphyrins undergo only porphyrin ring (ligand) centered redox reactions [22,54].

The cyclic voltammetric experiments were carried out using tetrabutylammonium perchlorate (TBAP) as supporting electrolyte in inert atmosphere. The compound shows two reversible oxidation peaks. The first peak at $E_{1/2} = 0.69$ V (vs. Ag/AgCl) is due to the one electron oxidation of porphyrin to form porphyrin π -cation radical $[\text{Mg}(\text{TDMPP})]^+$ and the second oxidation peak at 0.91 V vs

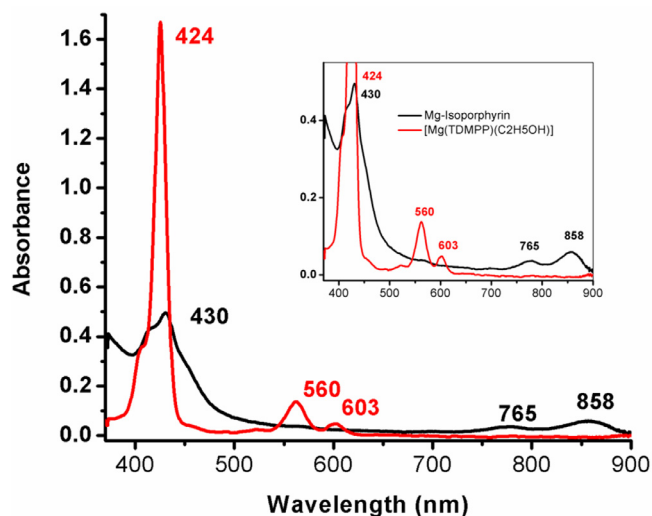


Fig. 3. Electronic spectrum of $[\text{Mg}(\text{TDMPP})(\text{C}_2\text{H}_5\text{OH})]$, (red trace) and on addition of CAN, (black trace).

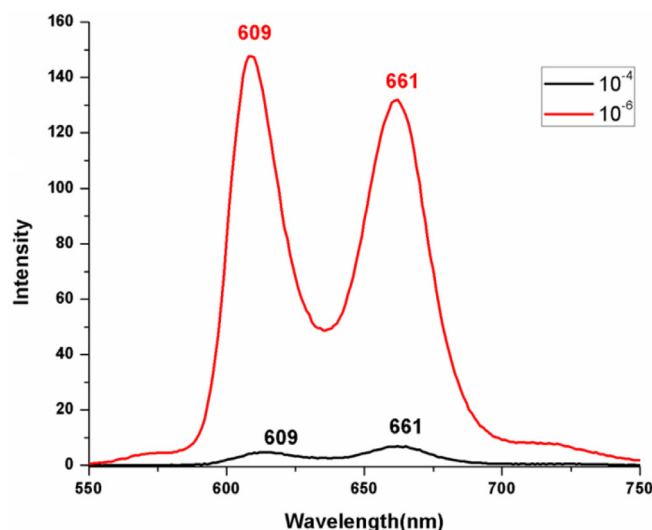


Fig. 4. Luminescence spectra of the compound 1 at concentration 10^{-6} M (red trace) and 10^{-4} M (black trace) in dichloromethane ($\lambda_{\text{ex}} = 420$ nm).

Ag/AgCl is due to formation of porphyrin dication $[\text{Mg}(\text{TDMPP})]^{++}$ (Fig. 5). The lower oxidation potential supports the oxidation of compound to its dication $[\text{Mg}(\text{TDMPP})]^{++}$ by chemical oxidants like ceric ammonium nitrate (CAN) and subsequent conversion to magnesium isoporphyrin.

Theoretical calculations

The geometry of compound $[\text{Mg}(\text{TDMPP})(\text{C}_2\text{H}_5\text{OH})]$ and $[\text{Zn}(\text{TDMPP})(\text{C}_2\text{H}_5\text{OH})]$ were optimized by DFT method using basis set LANL2DZ [28] along with functional B3LYP [29,30]. Using the geometrically optimized structure electronic energy for the compound was calculated to investigate the electronic property intensively and to understand the contributions to chemical bonding of metal center as well as surrounding ligand part by the TD-SCF (Time Depending- Self Consistent Field) method. The partial molecular energy level diagram has been derived from the electronic energy calculation using the contours of selective frontier orbitals (HOMOs-LUMOs) and is shown in Fig. 6. From the energy level diagram, it is found that metal center and axially bound ethanol moiety does not have significant contribution towards the

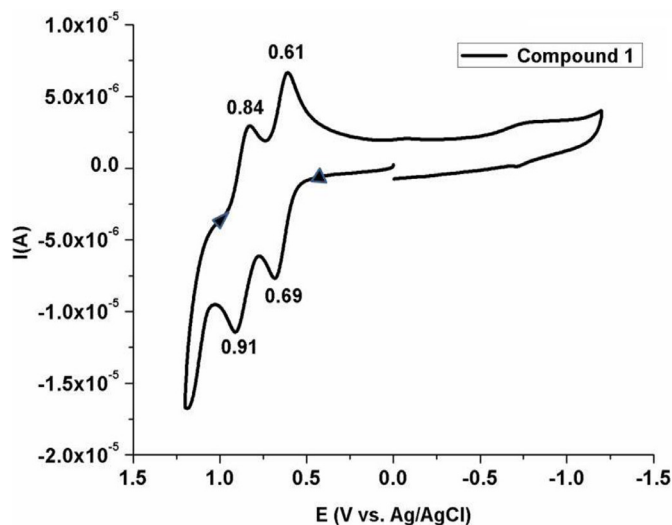


Fig. 5. Cyclic voltammogram of compound $[\text{Mg}(\text{TDMPP})(\text{C}_2\text{H}_5\text{OH})]$ in dichloromethane.

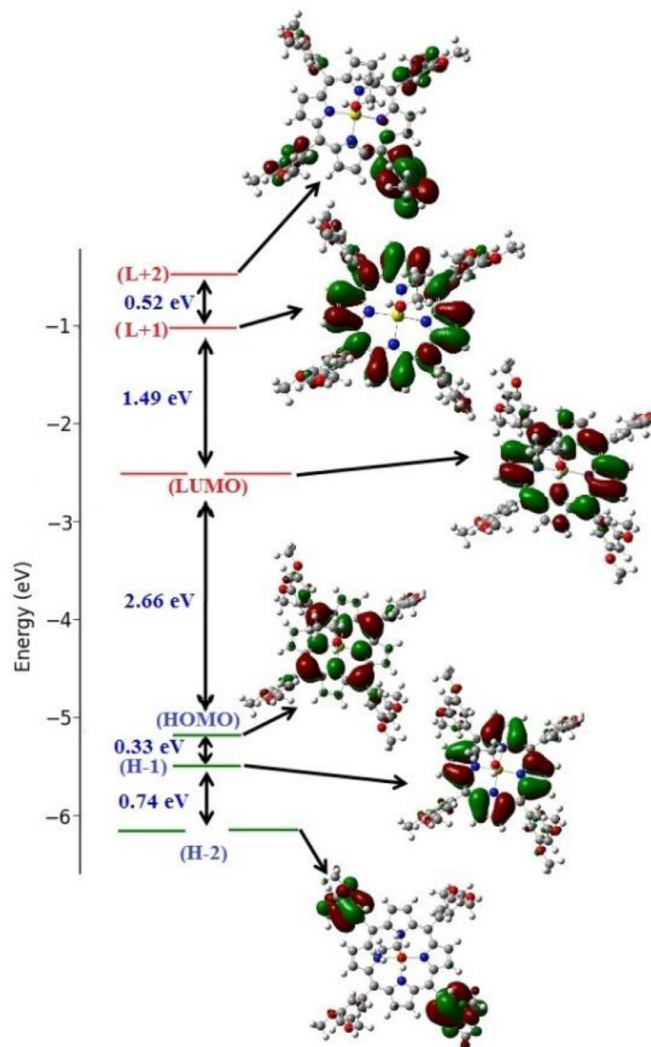


Fig. 6. Frontier molecular orbital energy level diagram of compound $[\text{Mg}(\text{TDMPP})(\text{C}_2\text{H}_5\text{OH})]$

Table 3
Comparison of experimental and theoretical bond parameters of [Mg(TDMPP)(C₂H₅OH)], **1**.

Bond	Experimental(Å)	Theoretical(Å)	Angle	Experimental(°)	Theoretical(°)
Mg-N1	2.080(2)	2.087	N1-Mg-N2	88.77(8)	89.364
Mg-N2	2.075(2)	2.086	N1-Mg-N4	88.38(8)	88.694
Mg-N3	2.076(2)	2.083	N3-Mg-N4	88.77(8)	89.614
Mg-N4	2.079(2)	2.085	N3-Mg-N2	88.56(8)	88.623
Mg-O9 _(ethanol)	2.079(2)	2.091	N1-Mg-N3	162.683	165.066
			Mg1-O9-C53	128.2(2)	128.912
			N1-Mg-O9	98.760	97.056

frontier molecular orbitals (FMOs) as the metal center magnesium has no d-orbital. The energy difference between HOMO and LUMO for compound **1** is found to be as 2.66 eV which is responsible for the lowest energy transition at 604 nm. The HOMO orbital is mainly contributed by the four nitrogen *P_z* orbitals of pyrrole whereas the LUMO orbitals are predominantly constructed by the π -bond character of pyrrolic carbons.

Some selective bond lengths and bond angles have been tabulated in Table 3 with their experimental and calculated values. The values agree well with the experimental data obtained from the crystal structure. These values are also in agree with less deviation with earlier reported magnesium porphyrin complexes [15,16,39,40]. The calculated UV-Visible spectrum shows three bands, the intense Soret band (at about 420 nm) and two Q-bands at around 565 nm similar to the experimental spectrum with slight variation from experimental λ_{max} values. The calculated and experimental UV-Visible spectrum of the compound is shown in supplementary information as Fig S6.

Global reactivity indices

Employing the energy calculation data of the optimized structure of the Mg-porphyrin and zinc porphyrin the global reactivity indices were calculated to understand the differences between zinc and magnesium porphyrins. The chemical hardness (η) [55] and chemical potential [56] (μ) were calculated utilizing the following equations as mentioned below and subsequently the value of chemical electrophilicity index [57] (ω) was calculated. And the softness (*s*) is $\frac{1}{\eta}$.

$$\text{Chemical hardness, } \eta = \frac{E_{\text{LUMO}} - E_{\text{HOMO}}}{2} \quad (1)$$

$$\text{Chemical potential, } \mu = \frac{E_{\text{LUMO}} + E_{\text{HOMO}}}{2} \quad (2)$$

$$\text{Global electrophilicity index, } \omega = \frac{\mu^2}{\eta} \quad (3)$$

The chemical hardness describes the reactivity and hence the stability of the chemical species; it is a measure of resistance to changes in its electronic configuration. Chemical potential is the correlation between the electronic energy changes according to the number of electrons involved during the charge transfer. The parameter global electrophilicity index is important which describes the maximum energetic stabilization of a chemical species that arises from accepting electronic charge. It is a positive quantity which describes the tendency of the electrophile to get an extra electronic charge determined by the chemical potential, μ . Since an electrophile is capable of accommodating electrons, its energy decreases when it accepts an electron and hence chemical potential is negative, but hardness is positive. Very limited study is known for the chemical reactivity indices of magnesium porphyrins [58–60].

The chemical parameters η , μ and ω for both Zn and Mg porphyrin complexes are obtained from the above mentioned equa-

Table 4

The global reactivity indices for compound **1** and **2**, (η -Chemical hardness, *s*-chemical softness, μ -chemical potential, ω -global electrophilicity index).

Compound	η (eV)	<i>s</i> (eV)	μ (eV)	ω (eV)
Mg(DMTTPP)(EtOH)	1.3298	0.752	-3.841	11.094
Zn(DMTTPP)(EtOH)	1.3389	0.747	-3.521	9.259

tions using HOMO-LUMO energies, and are listed in Table 4. Chemical hardness, η of Zn(DMTTPP)(EtOH) is slightly higher than Mg(DMTTPP)(EtOH), therefore Zn species is little a bit harder than the Mg complex. Similarly, the chemical potential, μ is found to be a bit higher negative for Mg complex. This may be due to presence of filled d orbital present in Zn metal. This values indicates that Mg(DMTTPP)(EtOH) is more reactive than Zn(DMTTPP)(EtOH) and suggests that magnesium porphyrin loses electron easily than zinc analogue. The parameter ω is smaller in case of Mg(DMTTPP)(EtOH) complex which means it is better electrophilic in nature than the corresponding Zn(DMTTPP)(EtOH) complex.

Hirshfeld surface analysis and fingerprint plots

Hirshfeld surfaces analysis and calculation of associated fingerprint region has recently become an indispensable approach to investigate intensively different type of strong as well as weak interactions present in the crystal lattice. The term Hirshfeld surface was given in honour to F. L. Hirshfeld, who first used the “stockholder partitioning” model for defining atoms in molecules [61]. It divides the crystal space into molecular regions where aggregate electron distribution of spherical atoms for a molecule (procrystal) exceeds half of the total electron density of the crystal (procrystal) [62,63]. Weighing function $w(\mathbf{r})$ can be used to explain Hirshfeld surface, where $w(\mathbf{r}) \geq 0.5$. Here, $\rho_a(\mathbf{r})$ is spherically averaged electron density [62,63].

$$w(\mathbf{r}) = \sum_{a \in \text{molecule}} \rho_a(\mathbf{r}) / \sum_{a \in \text{crystal}} \rho_a(\mathbf{r}) = \rho_{\text{promolecule}}(\mathbf{r}) / \rho_{\text{procrystal}}(\mathbf{r}) \quad (4)$$

Fingerprint plots can be drawn from Hirshfeld surface and was introduced to remove the complication of displaying two dissimilar but important distances mapped on a three-dimensional molecular surface in a two-dimensional format. We have quantified various kinds of major interactions for the compound [Mg(TDMPP)(C₂H₅OH)] in crystal packing mode using this Hirshfeld surface analysis and correlated with 2D fingerprint plot. Besides that, different quantitative measurements like volume (*V_H*), surface area (*S_H*), globularity (*G*), asphericity (Ω) have also been analyzed. The globularity [64] is observed less than **1** indicating the more structured molecular surface not spherical.

The asphericity [65] was found as 0.091 showing isotropic nature of the structure. The red specified spot in the *d_{norm}* surface, Fig. 7(a), reveals a strong hydrogen bonding interaction between axially coordinated O-H group of ethanol with the O-atom of neighboring *m*-OCH₃ group of successive Mg-porphyrin moiety and the faint red or white spots denote comparatively weaker

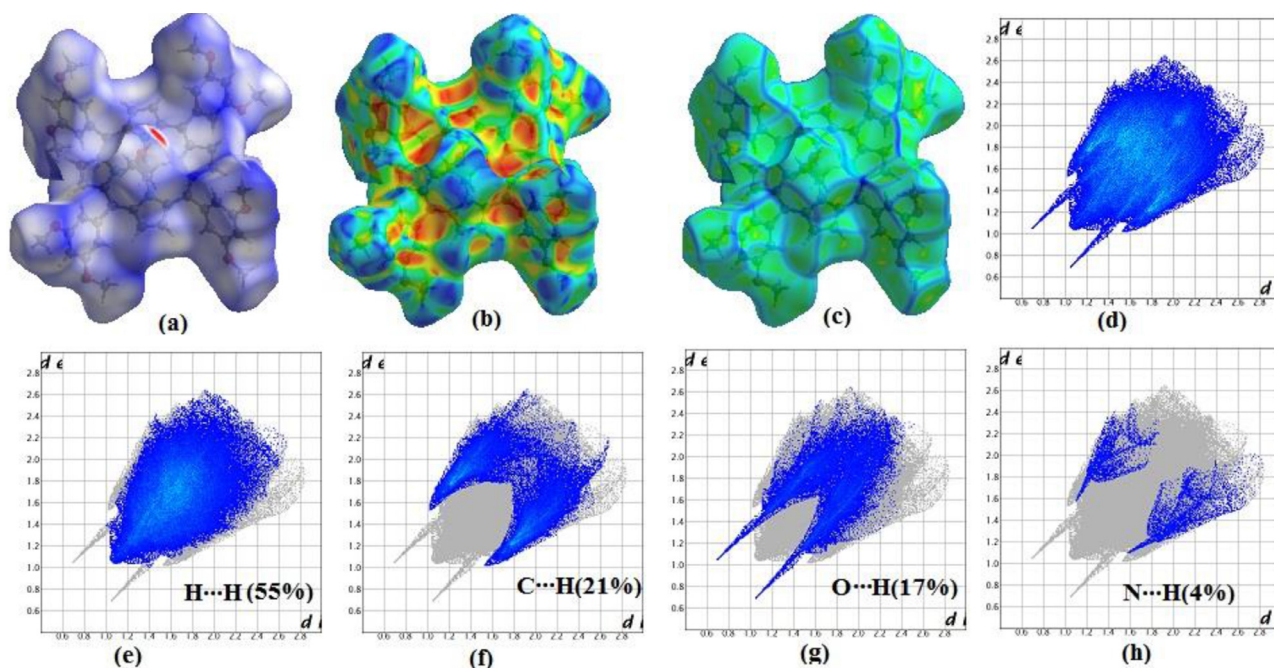


Fig. 7. Different types of Hirshfeld surfaces of compound $[\text{Mg}(\text{TDMPP})(\text{C}_2\text{H}_5\text{OH})]$ mapping with (a) d_{norm} ranging from -0.5 \AA (red) to 1.75 \AA (blue), (b) shape-index, (c) curvedness, (d) 2D fingerprint plot for compound $[\text{Mg}(\text{TDMPP})]$ with d_e vs. d_i (e), (f), (g) and (h) are showing d_e vs. d_i for H...H, C...H, O...H, and N...H interaction respectively with percentage.

dispersive interactions. Shape index and curvedness surface analysis also provide information about the crystal packing modes and short contacts. The orange concave regions in shape index, Fig. 7(b), are due to the acceptor atoms present in crystal whereas the blue regions for donor H-atoms. In Fig. 7(c) the curvedness is shown, which is a function of root mean square of surface of the crystal, indicating no flat surface. It appears there exists no stack type interaction in the crystal packing. Calculation of 2D fingerprint plot of d_i vs d_e represents various kinds of respective short contacts contributions in percentage towards the Hirshfeld surface [Fig. 7(d)]. From the analysis it is evident that the largest contribution is from the H...H contact which is equivalent to 55% [Fig. 7(e)]. Apart from this some other interactions like C...H, O...H, N...H are also present in the crystal as shown in (f), (g), (h) respectively of Fig. 7.

Conclusions

An ethanol bound magnesium porphyrin $[\text{Mg}(\text{TDMPP})(\text{C}_2\text{H}_5\text{OH})]$ have been synthesized and characterized using conventional spectroscopic methods along with single crystal X-ray diffraction method. The crystal structure reveals that the compound shows one dimensional weak H-bonding supramolecular structure due to axial ethanol molecule and a methoxy group of an adjacent porphyrin. The electrochemistry showed two reversible oxidation peaks at $E_{1/2} = 0.69 \text{ V}$ and 0.91 V vs Ag/AgCl respectively due to porphyrin ligand oxidation to form π -cation radical and dictation. Theoretical calculation was done using DFT method for magnesium porphyrin and its zinc analogue. Furthermore, the disadvantages of using zinc porphyrin for the study of magnesium porphyrin is computationally explored in this work comparing the global reactivity indices like η , μ and ω derived from theoretical calculations for zinc and magnesium porphyrins. Theoretical calculations support that magnesium porphyrin is more reactive than zinc porphyrins. These results of this work might have implications in the further study of reactivity differences between magnesium and similar biologically relevant

non-redox metallo-porphyrins. Hirshfeld surface analysis was also performed to quantify the intramolecular interactions present in the crystal structure.

Declaration of Competing Interest

The authors declare that they have no known competing financial interests or personal relationships that could have appeared to influence the work reported in this paper.

CRediT authorship contribution statement

Bishnu Prasad Borah: Investigation, Visualization, Writing - original draft. **Smita Majumder:** Investigation, Software, Visualization. **Karishma Devi Borah:** Software, Validation. **Jagannath Bhuyan:** Conceptualization, Writing - review & editing.

Acknowledgments

SM acknowledge national postdoctoral fellowship (NPDF,PDF/2017/000865) from SERB, DST. The work was supported by the project (MTR/2019/000223) from SERB, DST, New Delhi. Authors are thankful to Gauhati University, Guwahati, Assam for single crystal X-ray diffraction data.

Supplementary materials

Supplementary material associated with this article can be found, in the online version, at doi:[10.1016/j.molstruc.2020.129646](https://doi.org/10.1016/j.molstruc.2020.129646).

References

- [1] R. Paolesse, S. Nardis, D. Monti, M. Stefanelli, C.D. Natale, Porphyrinoids for chemical sensor applications, *Chem. Rev.* 117 (2017) 2517–6b00361, doi:[10.1021/acs.chemrev](https://doi.org/10.1021/acs.chemrev).
- [2] M.L. Merlau, W.J. Grande, S.T. Nguyen, J.T. Hupp, Enhanced activity of manganese(III) porphyrin epoxidation catalysts through supramolecular complexation, *J. Mol. Catal. A. Chem.* 156 (2000) 79, doi:[10.1016/S1381-1169\(99\)00399-4](https://doi.org/10.1016/S1381-1169(99)00399-4).

- [3] T. Ema, Y. Miyazaki, J. Shimonishi, C. Maeda, J. Hasegawa, Bifunctional porphyrin catalysts for the synthesis of cyclic carbonates from epoxides and CO₂: Structural optimization and mechanistic study, *J. Am. Chem. Soc.* 136 (2014) 15270, doi:10.1021/ja507665a.
- [4] N. Amiri, F.B. Taheur, S. Chevreux, E. Wenger, G. Lemercier, H. Nasri, Synthesis, crystal structure and spectroscopic characterizations of porphyrin-based Mg(II) complexes-Potential application as antibacterial agent, *Tetrahedron* 73 (2017) 7011, doi:10.1016/j.tet.2017.10.029.
- [5] S. Kladsomboon, T. Kercharoen, A method for the detection of alcohol vapours based on optical sensing of magnesium 5,10,15,20-tetraphenyl porphyrin thin film by an optical spectrometer and principal component analysis., *Anal. Chim. Acta.* 757 (2012) 75, doi:10.1016/j.aca.2012.10.054.
- [6] D.F. Oshea, M.A. Miller, H. Matsueda, J.S. Lindsey, Investigation of the scope of heterogeneous and homogeneous procedures for preparing magnesium chelates of porphyrins, hydrophorphyrins, and phthalocyanines, *Inorg. Chem.* 35 (1996) 7325, doi:10.1021/ic960812p.
- [7] J. Zhang, P. Zhang, Z. Zhang, X. Wei, Spectroscopic and kinetic studies of photochemical reaction of magnesium tetraphenylporphyrin with oxygen, *J. Phys. Chem. A* 2009 (2009) 5367, doi:10.1021/jp811209k.
- [8] K.D. Borah, J. Bhuyan, Magnesium porphyrins with relevance to chlorophylls, *Dalton Trans* 46 (2017) 6497, doi:10.1039/C7DT00823F.
- [9] F. D'Souza, M.E. El-Khouly, S. Gadde, A.L. McCarty, P.A. Karr, M.E. Zandler, Y. Araki, O. Ito, Self-assembled via axial coordination magnesium porphyrin-imidazole appended fullerene dyad: spectroscopic, electrochemical, computational, and photochemical studies *J. Phys. Chem. B.* 109 (2005) 10107, doi:10.1021/jp050591i.
- [10] J. Bhuyan, R. Sarkar, S. Sarkar, A Magnesium porphyrin bicarbonate complex with CO₂-modulated photosystem I action, *Angew. Chem. Int. Ed.* 50 (2011) 10603, doi:10.1002/ange.201103876.
- [11] M. Nappa, J.S. Valentine, The influence of axial ligands on metalloporphyrin visible absorption spectra. Complexes of tetraphenylporphyrinatozinc, *J. Am. Chem. Soc.* 100 (1978) 5075, doi:10.1021/ja00484a027.
- [12] S. Lipstman, I. Goldberg, Versatile supramolecular reactivity of zinc-tetra(4-pyridyl)porphyrin in crystalline solids: Polymeric grids with zinc dichloride and hydrogen-bonded networks with mellicitic acid, *Beilstein, J. Org. Chem.* 5 (2009) 1, doi:10.3762/bjoc.5.77.
- [13] H.M. Titi, B.K. Tripuramallu, I. Goldberg, Porphyrin-based assemblies directed by non-covalent interactions: highlights of recent investigations, *Cryst. Eng. Comm.* 18 (2016) 3318, doi:10.1039/C6CE00359A.
- [14] K.D. Borah, N.G. Singh, J. Bhuyan, Magnesium trimethoxyphenylporphyrin chain controls energy dissipation in the presence of cholesterol, *J. Chem. Sci.* 129 (2017) 449, doi:10.1007/s12039-017-1251-0.
- [15] D.R. Zbik, M. Witk, L. Fiedor, Ligand of water to magnesium chelates of biological importance, *J. Mol. Model* 19 (2013) 4661, doi:10.1007/s00894-012-1459-3.
- [16] J. Bhuyan, S. Sarkar, Self-assembly of magnesium and zinc trimethoxyphenylporphyrin polymer as nanospheres and nanorods, *Cryst. Growth Des.* 11 (2011) 5410, doi:10.1021/cg2010002.
- [17] K. Ezzayani, S. Nasri, M.S. Belkhiria, J.C. Daran, H. Nasri, Diaqua(5,10,15,20-tetraphenylporphyrinato-[kappa]4N)magnesium-18-crown-6 (1/1), *Acta Cryst. Sec. E* 69 (2013) m114, doi:10.1107/S1600536813001219.
- [18] N. Amiri, M. Hajji, T. Roisnel, G. Simonneaux, H. Nasri, Synthesis, molecular structure, photophysical properties and spectroscopic characterization of new 1D-magnesium(II) porphyrin-based coordination polymer, *Res. Chem. Intermed.* 44 (2018) 5583, doi:10.1007/s11664-018-3442-9.
- [19] S. Yang, R.A. Jacobson, Synthesis, crystal structure and molecular modeling of aquo magnesium tetra(methoxyphenyl)porphyrin, *Inorg. Chim. Acta* 190 (1991) 129, doi:10.1016/S0020-1693(00)80241-8.
- [20] S.K.A. Ikbal, S. Brahm, S.P. Rath, Building-up remarkably stable magnesium porphyrin polymers self-assembled via bidentate axial ligands: Synthesis, structure, surface morphology, and effect of bridging ligands, *Inorg. Chem.* 5118 (2012) 9666, doi:10.1021/ic300826p.
- [21] C. Stangel, A. Charisiadis, G.E. Zervaki, V. Nikolaou, G. Charalambidis, A. Kahnt, G. Rotas, N. Tagmatarchis, G.A. Coutsolelos, A case study for artificial photosynthesis: Non-covalent interactions between c60 dipyrrolyl and zinc porphyrin dimer, *J. Phys. Chem.* 121 (2017) 4850, doi:10.1021/acs.jpcc.6b11863.
- [22] N.G. Singh, K.D. Borah, S. Majumder, J. Bhuyan, Ethanol coordinated zinc trimethoxyphenylporphyrin: structure, theoretical studies and formation of isoporphyrin, *J. Mol. Struct.* 1200 (2020) 127116, doi:10.1016/j.molstruc.2019.127116.
- [23] P. Bhyrappa, S.R. Wilson, K.S. Suslick, Hydrogen-bonded porphyrinic solids: Supramolecular networks of octahydroxy porphyrins, *J. Am. Chem. Soc.* 119 (1997) 8492, doi:10.1021/ja971093w.
- [24] P. Bhyrappa, C. Arunkumar, J.J. Vittal, Synthesis and crystal structure of 5-(4-carboxyphenyl)-10,15,20-tri(4-*t*-butylphenyl)porphyrinato zinc(II) complex, *J. Chem. Sci* 117 (2005) 139, doi:10.1007/BF03356108.
- [25] J.J. McKinnon, D. Jayatilaka, M.A. Spackman, Towards quantitative analysis of intermolecular interactions with hirshfeld surfaces, *Chem. Commun* 37 (2007) 3814, doi:10.1039/B704980C.
- [26] O.V. Dolomanov, L.J. Bourhis, R.J. Gildea, J.A.K. Howard, H. Puschmann OLEX2, A complete structure solution, refinement and analysis program, *J. Appl. Cryst.* 42 (2009) 339, doi:10.1107/S0021889808042726.
- [27] Gaussian 16, Revision C.01, M.J. Frisch, G.W. Trucks, H.B. Schlegel, G.E. Scuseira, M.A. Robb, J.R. Cheeseman, J.J. Montgomery, V. Barone, G.A. Petersson, H. Nakatsuji, X. Li, M. Caricato, A. Marenich, J. Bloino, B.G. Janesko, R. Gomperts, B. Mennucci, H.P. Hratchian, J.V. Ortiz, A.F. Izmaylov, J.L. Sonnenberg, D. Williams-Young, F. Ding, F. Lipparini, F. Egidi, J. Goings, B. Peng, A. Petrone, T. Henderson, D. Ranasinghe, V.G. Zakrzewski, J. Gao, N. Rega, G. Zheng, W. Liang, M. Hada, M. Ehara, K. Toyota, R. Fukuda, J. Hasegawa, M. Ishida, T. Nakajima, Y. Honda, O. Kitao, H. Nakai, T. Vreven, K. Throssell, J.A.J.R. Montgomery, J.E. Peralta, F. Ogliaro, M. Bearpark, J.J. Heyd, E. Brothers, K.N. Kudin, V.N. Staroverov, T. Keith, R. Kobayashi, J. Normand, K. Raghavachari, A. Rendell, J.C. Burant, S.S. Iyengar, J. Tomasi, M. Cossi, J.M. Millam, M. Klene, C. Adamo, R. Cammi, J.V. Ochterski, R.L. Martin, K. Morokuma, O. Farkas, J.B. Foresman, D.J. Fox, Gaussian, Inc, Wallingford CT, 2016
- [28] P.J. Hay, W.R. Wadt, Ab initio effective core potentials for molecular calculations. Potentials for main group elements Na to Bi, *J. Chem. Phys.* 82 (1985) 299, doi:10.1063/1.448800.
- [29] A.D. Becke, Density functional thermochemistry. III. The role of exact exchange, *J. Chem. Phys.* 98 (1993) 5648, doi:10.1007/s002149900065.
- [30] C. Lee, W. Yang, R.G. Parr, Development of the colle-salvetti correlation-energy formula into a functional of the electron density, *Phys. Rev. B* 37 (1988) 785, doi:10.1103/PhysRevB.37.785.
- [31] M. Sankar, P. Bhyrappa, B. Varghese, K.K. Praneeth, G. Vijayanthimala, Meso-tetrakis(3',5'-di-substituted-phenyl)porphyrins: structural, electrochemical and axial ligation properties, *J. Porphyrins Phthalocyanines* 9 (2005) 413, doi:10.1142/S1088424605000514.
- [32] S.K. Wolff, D.J. Grimwood, J.J. McKinnon, M.J. Turner, D. Jayatilaka, M.A. Spackman, *Crystal explorer 3* (2013) 1 University of Western Australia, Crawley, Western Australia, 2005–2013.
- [33] A.D. Adler, F.R. Longo, J.D. Finarelli, J. Goldmacher, J. Assour, Korsakoff L, A simplified synthesis for meso-tetraphenylporphine, *J. Org. Chem.* 32 (1967) 476, doi:10.1021/jo01288a053.
- [34] J.S. Lindsey, J.N. Woodford, A simple method for preparing magnesium porphyrins, *Inorg. Chem.* 34 (1995) 1063, doi:10.1021/ic00109a011.
- [35] R. Timkovich, A. Tulinsky, Structure of aquomagnesium tetraphenylporphyrin, *J. Am. Chem. Soc.* 91 (1969) 4430, doi:10.1021/ja01044a018.
- [36] H.S. Chow, R. Serline, C.E. Strouse, Crystal and molecular structure and absolute configuration of ethyl chlorophyllide a-dihydrate. model for the different spectral forms of chlorophyll a, *J. Am. Chem. Soc.* 97 (1975) 7230, doi:10.1021/ja00858a006.
- [37] A. Agostini, E. Meneghin, L. Gewehr, D. Pedron, D.M. Palm, D. Carbonera, H. Paulsen, E. Jaenicke, E. Collini, How water-mediated hydrogen bonds affect chlorophyll a/b selectivity in water-soluble chlorophyll protein, *Sci. Rep.* 9 (2019) 18255, doi:10.1038/s41598-019-54520-4.
- [38] A.B. Fredj, Z.B. Lakhdara, M.F. Ruiz-López, The structure of chlorophyll a-water complexes: insights from quantum chemistry calculations, *Chem. Commun* 718 (2008), doi:10.1039/B716800D.
- [39] A.P. Dove, V.C. Gibson, E.L. Marshall, A.J.P. White, D.J. Williams, Magnesium and zinc complexes of a potentially tridentate-diketiminato ligand, *Dalton Trans* 570 (2004), doi:10.1039/B314760F.
- [40] A. Ghosh, S.M. Mobin, R. Frohlich, R.J. Butcher, D.K. Maity, M. Ravikanth, Effect of five membered versus six membered meso-substituents on structure and electronic properties of Mg(II) porphyrins: a combined experimental and theoretical study, *Inorg. Chem.* 49 (2010) 8287, doi:10.1021/ic1008522.
- [41] M. Wońska, P.M. Dominiak, S. Grabowsky, K. Woźniak, D. Jayatilaka, Hydrogen atoms can be located accurately and precisely by x-ray crystallography, *Sci. Adv.* 2 (2016) e1600192, doi:10.1126/sciadv.1600192.
- [42] L.A. Malaspina, A.A. Hoser, A.J. Edwards, M. Wońska, M.J. Turner, J.R. Price, K. Sugimoto, E. Nishibori, H. Bürgi, D. Jayatilaka, S. Grabowsky, Hydrogen atoms in bridging positions from quantum crystallographic refinements: Influence of hydrogen atom displacement parameters on geometry and electron density, *Cryst. Eng. Comm.* 22 (2020) 4778, doi:10.1039/DOCE00378F.
- [43] Y.D. Wu, X.H. Liu, J. Xu, S. Zhang, K. Shen, L. Sun, Y.M. He, Y. Ma, A. Zhang, Crystal structure of an apremilast ethanol hemisolvate hemihydrate solvatomorph, *Acta Cryst E73* (2017) 821, doi:10.1107/S2056989017006661.
- [44] M. Gouterman, Spectra of porphyrins, *J. Mol. Spectrosc.* 6 (1961) 138, doi:10.1016/0022-2852(61)90236-3.
- [45] K.D. Borah, J. Bhuyan, Methoxy-isoporphyrins of water-soluble porphyrins: synthesis, characterization and electrochemical properties, *J. Coord. Chem.* 72 (2019) 2251, doi:10.1080/00958972.2019.1654092.
- [46] J. Bhuyan, Metalloisoporphyrins: from synthesis to applications, *Dalton Trans* 44 (2015) 15742, doi:10.1039/C5DT01544H.
- [47] J. Bhuyan, Nucleophilic ring-opening of iron(III)-hydroxy-isoporphyrin, *Dalton Trans* 45 (2016) 2694, doi:10.1039/C5DT03905C.
- [48] J. Bhuyan, S. Sarkar, NO₂-induced synthesis of nitrate-iron(III) porphyrin with diverse coordination mode and the formation of isoporphyrin, *J. Chem. Sci.* 125 (2013) 707, doi:10.1007/s12039-013-0447-1.
- [49] A. Harriman, Luminescence of porphyrins and metalloporphyrins, *J.C.S. Faraday I* 76 (1980) 1978, doi:10.1039/F19807601978.
- [50] S. Grenoble, M. Gouterman, G. Khalil, J. Calli, L. Dalton, Pressure-sensitive paint (PSP): concentration quenching of platinum and magnesium porphyrin dyes in polymeric films, *J. Lumin.* 113 (2005) 33, doi:10.1016/j.jlumin.2004.08.049.
- [51] T. Ichiki, Y. Matsuo, E. Nakamura, Photostability of a dyad of magnesium porphyrin and fullerene and its application to photocurrent conversion, *Chem. Commun.* 49 (2013) 279, doi:10.1039/C2CC36988E.
- [52] F. Li, S. Gentemann, W.A. Kalsbeck, J. Seth, J.S. Lindsey, D. Holten, D.F. Bocian, Effects of central metal ion (Mg, Zn) and solvent on singlet excited-state energy flow in porphyrin-based nanostructures, *J. Mater. Chem.* 7 (1997) 1245, doi:10.1039/A700146K.
- [53] T. Matsuura, K. Inoue, A.C. Ranade, I. Salto, Photooxygenation of magnesium

- meso*-tetraphenylporphyrin, Photochem. Photobiol. 31 (1979) 23, doi:[10.1111/j.1751-1097.1980.tb03677.x](https://doi.org/10.1111/j.1751-1097.1980.tb03677.x).
- [54] K.M. Kadish, E.V. Caemelbecke, Electrochemistry of porphyrins and related macrocycles, J. Solid State Electrochem. 7 (2003) 254, doi:[10.1007/s10008-002-0306-3](https://doi.org/10.1007/s10008-002-0306-3).
- [55] P.K. Chattaraj, S. Nath, A.B. Sannigrahi, Hardness, Chemical Potential and Valency Profiles of Molecules under Internal Rotations, J. Phys. Chem. 98 (1994) 9143, doi:[10.1021/j100088a009](https://doi.org/10.1021/j100088a009).
- [56] X.T. Feng, J.G. Yu, M. Lei, W.H. Fang, S. Liu, spectroscopy Structure, and reactivity properties of porphyrin pincers: A conceptual density functional theory and time-dependent density functional theory study, J. Phys. Chem. A 112 (2018) 305, doi:[10.1021/jp905885y](https://doi.org/10.1021/jp905885y).
- [57] R.G. Parr, L.V. Szentpaly, S. Liu, Electrophilicity Index, J. Am. Chem. Soc. 121 (1999) 1922, doi:[10.1021/ja983494x](https://doi.org/10.1021/ja983494x).
- [58] J. Frau, F. Muñoz, D.G. Mitnik, A conceptual DFT study of the chemical reactivity of magnesium octaethylporphyrin (MgOEP) as predicted by the Minnesota family of density functional, Quim. Nova. 40 (2017) 402, doi:[10.21577/0100-4042.20170004](https://doi.org/10.21577/0100-4042.20170004).
- [59] H. Kavousi, H. Raissi, A. Rezaeifard, M. Jafarpour, Stereoelectronic effects of porphyrin ligand on the oxygen transfer efficiency of high valent manganese-oxo porphyrin species: A DFT study, J. Porphyr. Phthalocyanines 19 (2015) 1, doi:[10.1142/S1088424615500881](https://doi.org/10.1142/S1088424615500881).
- [60] Y. Huang, A. Zhong, C. Rong, X. Xiao, S. Liu, Spectroscopy Structure, and Reactivity Properties of Porphyrin Pincers: A Conceptual Density Functional Theory and Time-Dependent Density Functional Theory Study, J. Phys. Chem. A 112 (2008) 305, doi:[10.1021/jp077178t](https://doi.org/10.1021/jp077178t).
- [61] F.L. Hirshfeld, Bonded-atom fragments for describing molecular charge densities, Theoret. Claim. Acta (Berl.) 44 (1977) 129, doi:[10.1007/BF00549096](https://doi.org/10.1007/BF00549096).
- [62] J.J. McKinnon, M.A. Spackman, A.S. Mitchell, Novel tools for visualizing and exploring intermolecular interactions in molecular crystals, Acta Cryst B60 (2004) 627, doi:[10.1107/S0108768104020300](https://doi.org/10.1107/S0108768104020300).
- [63] M.A. Spackman, D. Jayatilaka, Hirshfeld surface analysis, Cryst. Eng. Comm. 11 (2009) 19, doi:[10.1039/B818330A](https://doi.org/10.1039/B818330A).
- [64] A.Y. Meyer, The size of molecules, Chem. Soc. Rev. 15 (1986) 449, doi:[10.1039/CS9861500449](https://doi.org/10.1039/CS9861500449).
- [65] J. Rudnick, G. Gaspari, The asphericity of random walks, J. Phys. A: Math. Gen. 19 (1986) L191, doi:[10.1088/0305-4470/19/4/004](https://doi.org/10.1088/0305-4470/19/4/004).